

where

$$\Sigma_k \equiv \sigma_k - S\sigma_k S^{-1}.$$

Owing to (4f) this means that the operator  $\Sigma_k$  commutes with the four  $\beta_\mu$ ; it is therefore a multiple of the unit operator. Since, from (5d),  $\text{spur}\sigma_k=0$ , it follows that

$$S\sigma_k = \sigma_k S. \quad (\text{B5})$$

Hence by canonical transformation of (5c) one obtains

$$i\sigma_m = \beta_k \beta_l - \beta_l \beta_k.$$

The canonical transformation under consideration is characterized by

$$\beta_k \rightarrow \gamma_k, \quad \gamma_k \rightarrow \beta_k, \quad \sigma_k \rightarrow \sigma_k, \quad \beta_4 \rightarrow -\beta_4. \quad (\text{B6})$$

In Bhabha's five-dimensional scheme, using (16), this corresponds

to the transformation

$$x_k' = x_k, \quad x_4' = x_4, \quad x_5' = x_4, \quad (\text{B7})$$

i.e.,

$$a_1^1 = a_2^2 = a_3^3 = 1, \quad a_4^4 = a_5^4 = 1.$$

This describes a rotation through the angle  $\pi/2$  in the  $(x_4, x_5)$  plane, and reflection of  $x_5$ .

Owing to the relativistic covariance it is clear that any other  $\beta_k$  can play the role of  $\beta_4$ . Hence there are four transformations  $S_\mu$  such that

$$S_\mu \beta_\mu + \beta_\mu S_\mu = 0, \quad [S_\mu^2, \beta_\lambda] = 0. \quad (\text{B8})$$

It is interesting to note that  $S_\mu^2$  is now a multiple of the unit operator.

## Energy Release in the Disintegration of Be<sup>8</sup>

RICHARD R. CARLSON

*Department of Physics and Institute for Nuclear Studies, University of Chicago, Chicago, Illinois*

(Received July 26, 1950)

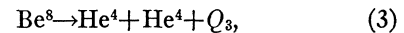
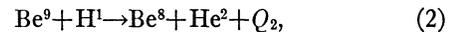
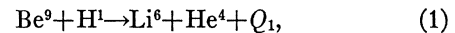
Thin beryllium targets were bombarded with 400-kev protons and the energy spectra of the particles given off at 90 degrees to the beam direction were observed with a cylindrical electrostatic analyzer. The beryllium was evaporated onto a nickel backing which was thin enough to confine the elastically scattered protons to a narrow energy range. At energies below that of the elastically scattered protons, peaks were observed in the energy spectra which corresponded to the maximum alpha-particle energy in the continuous energy distribution of alpha-particles resulting from the breakup of Be<sup>8</sup>. The position of these maxima give a value for the energy release in the disintegration of 77.5±4 kev.

### INTRODUCTION

THE nucleus Be<sup>8</sup> occurs as a compound state, or an intermediate product, in a large number of nuclear reactions.<sup>1</sup> In cases where the ground state is involved, there is evidence that alpha-decay occurs.<sup>2</sup> The result of the early work on this problem was the conclusion that the ground state of Be<sup>8</sup> was unstable against alpha-decay by about 125 kev. The conclusion, as to the instability of Be<sup>8</sup>, is bolstered by the fact that naturally occurring beryllium contains no detectable amount of mass eight isotope.<sup>3</sup> Recently, a measurement of the half-life for this decay was made by measuring the track lengths of fragments of oxygen nuclei in an emulsion when the emulsion had been exposed to energetic gamma-radiation.<sup>4</sup> Some of these fragments were identified as Be<sup>8</sup> nuclei. The half-life was found to be  $(5 \pm 1) \times 10^{-14}$  second. This value corresponds to an energy of the order of 100 kev which is available for decay into two alpha-particles, assuming

the latter have zero angular momentum.<sup>5</sup> Two recent direct measurements of the energy release give values of 103±10 kev,<sup>6</sup> and 89±4 kev.<sup>7</sup>

The method used in the present experiment, consisted in bombarding an evaporated beryllium target with protons. This results in the reactions,



where  $Q_1$ ,  $Q_2$ , and  $Q_3$  refer to the energy releases. Previous work has shown that the alpha-particles from reaction (3) have less energy than the elastically scattered protons at bombardment energies above 240 kev, where sufficient yields for our measurements may be expected.<sup>7,8</sup> In the present work, a backing of nickel foil was used, which was thin enough to confine the elastically scattered protons to a narrow range of energies, thus permitting alpha-particles to be observed without serious interference. An electrostatic analyzer was used to separate particles of different energy-to-charge ratio. In previous work with these reactions,

<sup>1</sup> Hornyak, Lauritsen, Morrison, and Fowler, *Revs. Modern Phys.* **22**, 309 (1950).

<sup>2</sup> Oliphant, Kempton, and Rutherford, *Proc. Roy. Soc. (London)* **150**, 241 (1935); O. Laaf, *Ann. Phys.* **32**, 743 (1938); K. Fink, *Ann. Phys.* **34**, 717 (1939); J. Wheeler, *Phys. Rev.* **59**, 27 (1941). Wheeler summarizes the earlier work and corrects some mistakes in analysis.

<sup>3</sup> A. Nier, *Phys. Rev.* **52**, 933 (1937).

<sup>4</sup> C. Miller and A. Cameron, *Phys. Rev.* **81**, 316 (1951).

<sup>5</sup> H. Bethe, *Revs. Modern Phys.* **9**, 167 (1937).

<sup>6</sup> A. Hemmendinger, *Phys. Rev.* **75**, 1267 (1949).

<sup>7</sup> Tollestrup, Fowler, and Lauritsen, *Phys. Rev.* **76**, 428 (1949).

<sup>8</sup> L. del Rosario, *Phys. Rev.* **74**, 304 (1948).

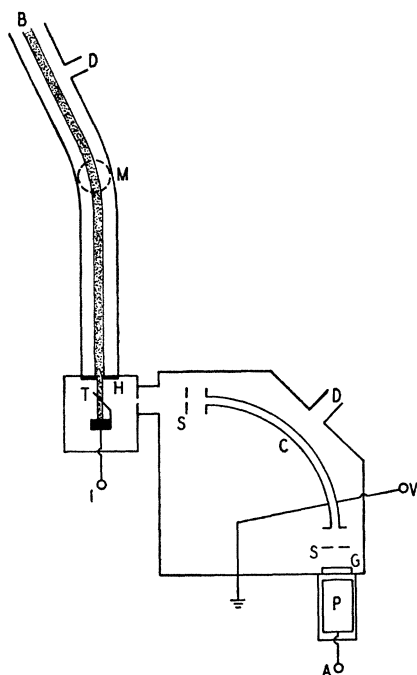


FIG. 1. Schematic diagram of experimental arrangement. A, connection to counting equipment; B, beam from kevatron; C, electrostatic analyzer plates; D, connection to diffusion pump; G, glass disk with zinc sulfide screen; H,  $\frac{1}{8}$ -inch collimating hole; I, connection to beam current integrator; M, magnetic field; P, photomultiplier tube; S, 0.1-cm slit; T, target; V, connection to high voltage.

particles of different momentum-to-charge ratio were separated and singly charged alpha-particles from the breakup of  $\text{Be}^8$  were observed with doubly charged lithium ions from the competing reaction being partially superposed.<sup>7</sup> Foils were used to separate the two ions. No stopping foils were used in the present arrangement.

In the course of this work, the lithium and deuterium ions, from the reactions indicated above, were observed and their energies measured. These measurements led to values for  $Q_1$  and  $Q_2$ . A great deal of work has been done on the measurement of these  $Q$  values and the values obtained here are of interest mainly in that they confirm the presently accepted results.<sup>7-9</sup>

#### DESCRIPTION OF THE APPARATUS

Figure 1 is a schematic diagram of the experimental arrangement. The various items are described below.

The source of the proton beam was the University of Chicago 400-kilovolt Cockroft-Walton accelerator, or

kevatron. The kevatron beam was first magnetically analyzed and the proton component directed down a one meter tube to the target. A  $\frac{1}{8}$ -inch diameter collimating hole limited the beam cross section in front of the target. A beam current of the order of two microamperes on the target was usually used. The current was monitored by a beam current integrator of conventional design. Since the target and backing together were too thin to stop the beam, a piece of  $\frac{1}{8}$ -inch thick metal was mounted behind the target and both were connected electrically to the integrator. The target assembly could be rotated and moved along the axis coincident with the beam direction through a Wilson seal. By using this freedom of motion and a window looking into the target chamber, the position of the beam spot on the target was brought opposite the analyzer entrance. The positioning was checked by making sure it maximized the counting rate due to scattered protons. The direction of entrance to the analyzer was defined by the 0.1-cm slit and window as shown in the schematic; a finite acceptance angle of approximately 0.020 radian is also defined by the geometry of the layout. The angle between the beam and the direction of entrance to the analyzer was known to be 90 degrees to an accuracy of 0.5 degree, or 0.009 radian, from the accurate machining of the analyzer and target chamber parts.

The electrostatic analyzer used in this experiment has been described in the literature.<sup>10</sup> Briefly, it is of the cylindrical type with an average radius of 15 cm, spacing of 0.5 cm, and a deflection angle of 90 degrees. Voltages up to 50 kilovolts have been applied across the analyzer plates and for such voltages protons of 750-kev energy are focused. From the calibration experiments carried out in this laboratory, the analyzer constant for the arrangement employed was known to be 15.78<sub>8</sub>. The constant is the ratio of the energy in kilovolts per charge (in units of the electronic charge) of the ion focused to the voltage across the analyzer plates in kilovolts.

A scintillation screen was used to detect particles which managed to traverse the analyzer. The screen was made by putting a thin coating of activated zinc sulfide powder on a glass disk.<sup>11</sup> The scintillations were detected by an RCA 5819 photomultiplier tube using 900 volts of batteries for the voltage supply. Batteries were found necessary for adequate stability. The pulse output of the photomultiplier tube was fed through a preamplifier to an amplifier and thence to a discriminator and scalar; all were of the type described by Elmore and Sands.<sup>12</sup> An amplifier gain of about 320 was used throughout the entire work. With the arrangement used, it was found that, for voltages on the

<sup>9</sup> R. Döpel, *Z. Physik*, **91**, 796 (1934); F. Kirchner and H. Neuert, *Physik. Z.* **36**, 54 (1935); B. Zyrich, *Z. Physik*, **96**, 337 (1935); R. Döpel, *Z. Physik*, **104**, 666 (1937); F. Kirchner and H. Neuert, *Physik. Z.* **38**, 969 (1937); J. Allen, *Phys. Rev.* **51**, 182 (1937); Williams, Haxby, and Shepherd, *Phys. Rev.* **52**, 1031 (1937); G. Hatch, *Phys. Rev.* **54**, 165 (1938); Allison, Skaggs, and Smith, *Phys. Rev.* **54**, 171 (1938); L. Skaggs, *Phys. Rev.* **56**, 24 (1939); Allison, Graves, Skaggs, and Smith, *Phys. Rev.* **57**, 550 (1940); Strait, Van Patter, Buechner, and Sperduto, *Phys. Rev.* **81**, 747 (1951).

<sup>10</sup> Allison, Frankel, Hall, Montague, Morrish, and Warshaw, *Rev. Sci. Instr.* **20**, 735 (1949).

<sup>11</sup> Patterson Type "D" Powder, E. I. du Pont Company.

<sup>12</sup> W. Elmore and M. Sands, *Electronics* (McGraw-Hill Book Publishing Company, Inc., New York, 1949).

Schmidt discriminator of 30 volts and over, the background counting rate was negligible.

The vacuum in the accelerator tube was maintained by an oil diffusion pump system. Liquid air traps between the pumps and the accelerator tube were used to keep oil vapor out of the tube during the time that measurements were made. To reduce the amount of oil deposition inside the accelerator tube, the connection between the pumping system and the accelerator tube was partly closed by a vane between runs. The problem of oil deposition on targets is acute in this experiment, since, as it will appear later, deposition is an important source of error for which very little can be done in the way of correction. To reduce the chance of oil deposition as much as possible, a liquid-air trap was placed on the vacuum pump used to rough-out the target chamber. Also, the target chamber was closed off from the accelerator tube and the analyzer between runs. The electrostatic analyzer had its own oil diffusion pump system and liquid air trap which was kept filled whenever the analyzer was open to the target chamber.

#### ENERGY MEASUREMENTS

The energy of the particles, which came off the target at right angles to the beam direction, was measured with the electrostatic analyzer. The voltage across the analyzer plates was measured by draining a small current through a 50 megohm stack of wirewound (Taylor) resistors of 0.1 percent precision. The drain was of the order of 200 microamperes. The meter, which was used to measure the drain, had an accuracy of 0.25 percent.

The voltage applied across the analyzer plates was obtained from a half-wave rectifier using 60-cycle, 110-volt input. A variac was used to vary the input to the step-up transformer of the rectifier; a Sola transformer was used to smooth out the line voltage fluctuations. A 0.05-microfarad condenser was used to reduce the ripple to 0.66 percent at the voltages used here.

From the calibration experiments, the analyzer constant was known to an accuracy of 0.1 percent; the analyzer resolution was known to be 0.33 percent. The analyzer had a triangular energy "window." That is to say, a monoenergetic group of particles would produce a triangular shaped energy spectrum with the maximum at the true energy and a width, at half-maximum, of 1/300 of the true energy if the voltage across the analyzer plates were perfectly steady. Actually there is a sawtooth ripple of 0.66 percent in the voltage. This causes the analyzer window to become roughly gaussian in shape with a width at half-maximum equal to the ripple. The effective window shape is drawn in Fig. 4B.

Including all the sources of inaccuracy discussed above, it is estimated that energy measurements with the analyzer on a monoenergetic group of particles could be made with an accuracy of 0.75 percent.

The accelerating voltage for the bombarding proton beam was measured by draining a small current from

the high voltage point of the kevatron through a resistor of approximately  $6.6 \times 10^9$  ohms. A Sola constant voltage transformer was used in the input to the kevatron. It is estimated that the kevatron accelerating voltage was maintained constant to within one part in five hundred from readings on the current drain. Previous work in this laboratory, by Morrish, showed that the kevatron has a total voltage fluctuation due to ripple of 2.1-kilovolts for a voltage of 330 kilovolts.<sup>13</sup> This was determined by measuring the energy spectrum of an H<sub>2</sub> beam sent directly into an electrostatic analyzer which had a voltage regulation better than that used in this experiment. A simplified analysis of the Cockroft-Walton circuit gives the ripple as 270 volts per 100 microamperes drain. This implies a drain of about 800 microamperes at a voltage of 330 kilovolts. Half of this is taken by the beam and the resistor drain. The remainder may be accounted for by leakage down supports, the glass accelerator tube, and tubes of kerosene coolant used in the ion source, and by corona loss.

As a result of the above mentioned work, a calibration table of the kevatron voltage against the current drain through the resistor stack was obtained. It is estimated that this table gives the accelerating voltage on the kevatron to an accuracy of one percent. For an accuracy of 0.1 percent, the calibration of the resistor stack against the electrostatic deflector must be carried out simultaneously with the measurement. An accuracy of one percent is quite adequate for the present work since an error of one percent in the bombarding energy contributes an error of a few tenths of a kilovolt in a total error of several kilovolts in the value of  $Q_3$ .

#### TARGET CHARACTERISTICS

The targets used in this experiment were prepared by vacuum evaporation, in the manner described by J. Strong, of beryllium onto thin nickel foils.<sup>14</sup> From the geometry of the evaporation set-up, the amount of beryllium put on the target was roughly estimated to be less than 0.005 mg/cm<sup>2</sup>. The nickel foils were obtained commercially in the form of  $\frac{1}{2}$ -inch squares.<sup>15</sup> The nickel had a nominal thickness of 1000 angstroms and was backed by copper of 2500-angstroms thickness. The manufacturer estimates the nickel thickness to be within  $\pm 20$  percent of the nominal value. From evidence discussed below, this would seem to be true of the average thickness. However, from the method of manufacture—electrodeposition of nickel upon a mandrel followed by electrodeposition of copper onto the nickel—one might expect thick spots in the foil. From evidence considered in the discussion of results, this would seem to be true also. The foils are quite sturdy in the form in which they are supplied; however,

<sup>13</sup> A. H. Morrish, *Phys. Rev.* **76**, 1651 (1949).

<sup>14</sup> J. Strong, *Procedures in Experimental Physics* (Prentice-Hall Company, New York, 1938).

<sup>15</sup> Chromium Corporation of America, Waterbury, Connecticut.

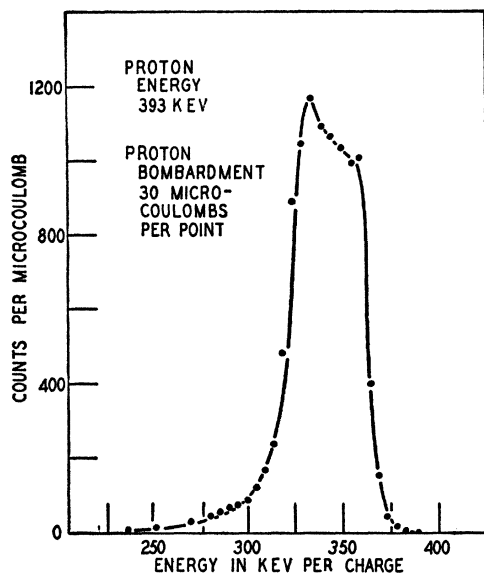


FIG. 2. Energy spectrum of elastically scattered protons.

any misuse will show up later as tears in the nickel. The nickel foil, with its backing on, was mounted in a holder. The assembly was dipped in a solution made up of roughly 50 percent concentrated ammonium hydroxide and 50 percent trichloroacetic acid by weight. The percentages are not critical. The copper dissolves in a few minutes whereas the nickel is unaffected. After stripping, the nickel foil was washed in two baths of distilled water for several hours. It is quite delicate at this stage and a jig is useful for handling purposes. Once the copper backing was stripped off, the foil was never removed from the holder. Bashkin and Goldhaber have recently described procedures of handling thin nickel foils quite similar to those used here.<sup>16</sup>

Figure 2 shows the energy spectrum obtained when 393-keV protons were elastically scattered at 90 degrees off one of the targets. Variation in detector efficiency and analyzer resolution with energy cannot modify the energy spectrum appreciably over the width of the scattered proton peak; consequently, the width at half-maximum should give the energy lost by protons in traveling through the foil a distance of  $2\sqrt{2}$  times the foil thickness. The factor  $2\sqrt{2}$  enters because the foil

was mounted so that the beryllium covered surface faced the analyzer entrance and the oncoming protons, and the perpendicular to this surface bisected the 90-degree angle between the beam direction and the direction of those particles entering the analyzer. The energy loss in this case was 41 keV. Using S. D. Warsaw's results on the rate of loss of energy by protons traversing various materials,<sup>17</sup> the estimated thickness of the nickel in this foil is 0.072 mg/cm<sup>2</sup> or 810 angstroms.

In Fig. 2, at an energy of 334 keV, there is a rise superimposed upon the main peak. This rise occurs at the place one would expect to find protons scattered by a carbon layer. This assignment is reasonable since the energy spectrum shown in Fig. 2 was measured on a target which had been subjected to about 25-microampere-hours of bombardment and exposed to untrapped diffusion pumps. Measurements of the energy of the alpha-particles from the breakup of Be<sup>8</sup> were never made under these circumstances; liquid air traps were always kept filled and targets were discarded for measurement purposes after about 6-microampere-hours bombardment, all of which was done in one run. The thickness of the carbon layer indicated in Fig. 2 may be calculated by using the fact that the position of the peak caused by scattering from nickel is lower than the expected value by 17 keV. Again using Warsaw's data, the beryllium layer can account for no more than 6 keV loss, leaving 11 keV to be lost in carbon by the protons in getting down to the top nickel layer and in getting out again. This gives the carbon thickness as about 0.01 mg/cm<sup>2</sup>. The protons scattered from the beryllium layer should, in Fig. 2, appear on the steep, low energy side of the peak scattered by nickel. The beryllium layer is so thin and its atomic number is so low that the protons it scatters are obscured in the rapidly falling slope of the nickel peak. For lower bombardment energies, peaks due to scattering from beryllium were observed.

#### FORMULAS FOR ENERGY RELEASES

For the nonrelativistic velocities involved in this experiment and for 90-degree observation, the laws of conservation of energy and momentum give the following formulas:

$$Q_1 = (1 + M_{Li}/M_\alpha)E_{Li} - (1 - M_p/M_\alpha)E_p, \quad (4)$$

$$Q_2 = (1 + M_d/M_{Be})E_d - (1 - M_p/M_{Be})E_p, \quad (5)$$

where "E" refers to the energy and "M" refers to the mass of the ion indicated by the subscript, whose meaning is indicated in Table I.

Neglecting for the moment the energy loss of the ions in the target material, Be<sup>8</sup> nuclei will give rise to a continuous distribution of alpha-particles with energies ranging from zero on up to a maximum value,  $E_\alpha$ . The origin of the continuous distribution lies in the fact that

TABLE I. Nuclear masses used in the calculations.

Nucleus	Symbol	Mass* (mass units on the physical scale)
H <sup>1</sup>	$M_p$	1.008
H <sup>2</sup>	$M_d$	2.015
He <sup>4</sup>	$M_\alpha$	4.004
Li <sup>6</sup>	$M_{Li}$	6.017
Be <sup>8</sup>	$M_{Be}$	8.008
Be <sup>9</sup>	$M_t$	9.015

\* See reference 18.

<sup>16</sup> S. Bashkin and G. Goldhaber, Rev. Sci. Instr. 22, 112 (1951).

<sup>17</sup> S. D. Warsaw, Phys. Rev. 76, 1759 (1949).

the alpha-particles are emitted in all directions with respect to the Be<sup>8</sup> nuclei, which may have any direction in the laboratory. From Fig. 3, which is a scale drawing of the velocity vectors involved in reactions (2) and (3), it may be seen that the maximum observed alpha-particle velocity, for 90-degree observation of the distribution, is given by,

$$v_\alpha^2 = (v_{\text{Be}} + v_\alpha')^2 - v_{\text{c.m.}}^2, \quad (6)$$

where  $v_\alpha$  is the observed alpha-particle velocity in the laboratory,  $v_{\text{Be}}$  is the velocity of the Be<sup>8</sup> ion in the center-of-mass system,  $v_\alpha'$  is the velocity of the alpha-particle with respect to the Be<sup>8</sup> ion, and  $v_{\text{c.m.}}$  is the velocity of the center of mass. If one substitutes the energies of the particles into Eq. (6) and solves for the energy release in the Be<sup>8</sup> breakup, one obtains,

$$Q_3 = 2 \left[ \{ E_\alpha + E_p M_p M_\alpha / (M_p + M_i)^2 \}^{\frac{1}{2}} - \{ Q_2 M_d M_\alpha / M_{\text{Be}} (M_{\text{Be}} + M_d) + E_p M_d M_\alpha M_i / M_{\text{Be}} (M_{\text{Be}} + M_d) (M_i + M_p) \}^{\frac{1}{2}} \right]^2. \quad (7)$$

Table I gives the values of the masses used in formulas (4), (5), and (7).<sup>18</sup> Exact values of for the masses have been used in these formulas but no corrections for relativistic effects have been made. This was considered justified since the Be<sup>8</sup> nucleus, which gives off the alpha-particle, has a velocity of  $1.9 \times 10^8$  cm/sec in the laboratory and the alpha-particle, a velocity of  $1.4 \times 10^8$  cm/sec with respect to the Be<sup>8</sup> nucleus. For these velocities, relativistic correction terms would be of the order of 0.01 percent and, consequently, negligible.

For observations taken at angles deviating from  $\frac{1}{2}\pi$  radians by a small amount  $\epsilon$ , corrections to formulas (4) and (5) become,

$$\Delta Q_1 = (4E_{\text{Li}} E_p M_{\text{Li}} M_p / M_\alpha^2)^{\frac{1}{2}} \epsilon, \quad (8)$$

$$\Delta Q_2 = (4E_d E_p M_d M_p / M_{\text{Be}}^2)^{\frac{1}{2}} \epsilon, \quad (9)$$

respectively. Corrections to formula (7) may be made by noticing that, to the first order in  $\epsilon$ ,

$$E_\alpha' = E_\alpha + \{ 4E_\alpha E_p M_\alpha M_p / (M_i + M_p)^2 \}^{\frac{1}{2}} \epsilon, \quad (10)$$

where  $E_\alpha'$  is the maximum alpha-particle energy at an angle to the beam of  $\frac{1}{2}\pi - \epsilon$  radians. If we replace  $E_\alpha$  by  $E_\alpha'$  in the second term on the right, substitute into formula (7), and expand to the first order in  $\epsilon$ , we get a correction to  $Q_3$  as follows

$$\Delta Q_3 = (1 - 1/S) \{ 4E_\alpha' E_p M_\alpha M_p / (M_i + M_p)^2 \}^{\frac{1}{2}} \epsilon, \quad (11)$$

$$S = \{ E_\alpha' + E_p M_\alpha M_p / (M_i + M_p)^2 \}^{\frac{1}{2}} \times \{ [Q_2 + E_p M_i / (M_i + M_p)] \times [M_d M_\alpha / M_{\text{Be}} (M_{\text{Be}} + M_d)] \}^{-\frac{1}{2}}. \quad (12)$$

These corrections are of interest because the finite acceptance angle of the analyzer introduces a spread in

the energy spectra and because deviation of the mean entrance angle from 90-degrees introduces a systematic source of error. It turns out that the spread due to the acceptance angle is comparable to that due to the analyzer ripple and, therefore, adds to the probable error. If the machining of the analyzer and target chamber parts was as good as claimed, there should be no systematic error of any importance arising from lack of knowledge of the mean entrance angle. Evidence in favor of this conclusion will be considered in the discussion of results obtained.

In order to estimate the effects of errors in the values of  $E_{\text{Li}}$ ,  $E_\alpha$ ,  $E_d$ ,  $E_p$ , and  $Q_2$  on the values of  $Q_1$ ,  $Q_2$ , and  $Q_3$ , the following formula was used

$$P_f^2 = \sum_i (\partial f(x_i) / \partial x_i)^2 P_i^2, \quad (13)$$

where  $P_f$  denotes the probable error in a quantity " $f$ ," which is a function of certain other quantities " $x_i$ ," which have probable errors  $P_i$ .<sup>19</sup> Application of formula

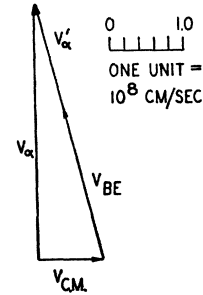


FIG. 3. Vector diagram of the velocities involved in reactions (2) and (3) under the conditions leading to maximum energy of the alpha-particles at 90-degrees to the proton beam.  $v_{\text{c.m.}}$  refers to the velocity of the center-of-mass system ( $\text{B}^{10}$ );  $v_{\text{Be}}$  refers to the velocity of the Be<sup>8</sup> ion in this center-of-mass system;  $v_\alpha'$  refers to the velocity of the alpha-particle, from the breakup of Be<sup>8</sup>, with respect to the Be<sup>8</sup> ion;  $v_\alpha$  refers to the velocity of the observed alpha-particle.

(13) to  $Q_3$  gives,

$$P_3 = 2(S - 1) \{ [P_\alpha/S]^2 + [P_2 M_d M_\alpha / M_{\text{Be}} (M_{\text{Be}} + M_d)]^2 + [M_d M_\alpha M_i / M_{\text{Be}} (M_{\text{Be}} + M_d) (M_i + M_p) - M_p M_\alpha / (M_p + M_i) S]^2 P_p^2 \}^{\frac{1}{2}}, \quad (14)$$

$$P_3 = 2(S - 1) \{ (P_\alpha/S)^2 + (P_2/10)^2 + (9 - 4/S)^2 (P_p/100)^2 \}^{\frac{1}{2}},$$

where  $P_\alpha$ ,  $P_2$ , and  $P_p$  are the probable errors in  $E_\alpha$ ,  $Q_2$ , and  $E_p$ , respectively.

#### ALPHA-PARTICLE DISTRIBUTION IN ENERGY

The experimentally observed energy spectrum will be influenced by various factors and some analysis is necessary to obtain the relation of the experimental observations to the nascent energy spectrum. First of all, if we consider a system in which the center of mass of the bombarding proton and the beryllium target nucleus is

<sup>18</sup> H. Bethe, *Elementary Nuclear Theory* (John Wiley and Sons, Inc., New York, 1947).

<sup>19</sup> H. Margenau and G. Murphy, *The Mathematics of Physics and Chemistry* (D. Van Nostrand Company, Inc., New York, 1943).

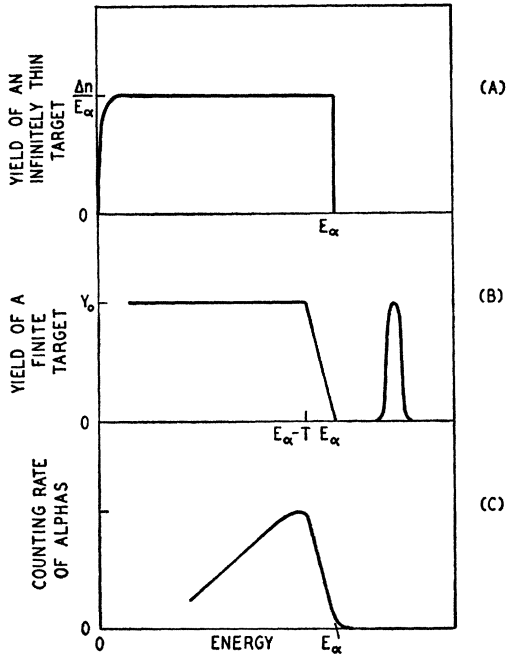


FIG. 4. A. Calculated energy spectrum of an infinitely thin target. B. Calculated energy spectrum of a finite target and the analyzer energy window. C. Calculated energy spectrum as modified by the analyzing and detecting equipment.

at rest, the distribution in energy of the alpha-particles from the breakup of  $\text{Be}^8$  is constant. This rests on the assumptions that  $\text{Be}^8$  is emitted with equal probability in all directions in the center of mass system and that alpha-particles are emitted isotropically with respect to the  $\text{Be}^8$ . The first assumption has been directly verified by measurements on the angular distribution of the deuterons.<sup>20</sup> The second assumption is quite reasonable since the ground state of  $\text{Be}^8$  is supposed to have zero angular momentum causing the alpha-particles to be emitted in an  $s$ -state.<sup>1</sup> Making these assumptions, one finds  $P(\mathbf{v})$ , the probability of a given velocity  $\mathbf{v}$ , for an alpha-particle, per unit volume of velocity space, to be,

$$P(\mathbf{v}) = \text{constant}/v. \quad (15)$$

Thus,

$$P(E)dE d\omega = P(v)v^2 dv d\omega, \quad P(E) = \text{constant}, \quad (16)$$

where  $P(E)$  is the probability per unit solid angle  $d\omega$ , of finding alpha-particles of energy  $E$ , in the center-of-mass system of the  $\text{B}^{10}$  compound nucleus. In the laboratory system of coordinates, one finds the corresponding quantities to be,

$$P(\mathbf{v}') = P(\mathbf{v}), \quad (17)$$

where  $P(\mathbf{v}')$  is the probability of a given velocity  $\mathbf{v}'$  in the laboratory, per unit volume of velocity space, for an alpha-particle, and  $\mathbf{v}$  and  $\mathbf{v}'$  refer to the same point

in velocity space with the prime referring to the laboratory system; thus,

$$P(E')dE'd\omega' = P(\mathbf{v}')v'^2 dv'd\omega' \\ = \text{constant} (v'/v)(v'dv')d\omega', \quad (18)$$

$$P(E') = \text{constant}(v'/v).$$

For 90-degree observation of alpha-particles, the resulting distribution is drawn in Fig. 4A for proton bombarding energies in our range.

For an infinitely thin target, the yield curve of Fig. 4A may be approximated by a step function and its area by a rectangle since it is the shape near  $E_\alpha$  that is of interest; this gives,

$$\Delta n = \int_0^{E_\alpha} Y(E)dE = 2\sigma F \Delta N, \quad (19)$$

Yield,  $Y(E) = (\Delta n/E_\alpha)$ ,

where  $E_\alpha$  is the maximum alpha-particle energy,  $\Delta n$  is the total number of alpha-particles produced,  $\sigma$  is the cross section,  $F$  is the proton flux, and  $\Delta N$  is the number of target nuclei. For thicker targets one must sum the contributions of many such layers to obtain the yield of alpha-particles of energy  $E'$ ,

$$Y(E') = \int_{E'}^{E_\alpha} dn/E = \int_{E'}^{E_\alpha} 2\sigma F dN/E, \quad (20)$$

$$dN = \text{constant}(dE/L), \quad (21)$$

where  $L$  is the rate of loss of energy of emergent ions in the target. If we assume that our target thickness to entrant and emergent ions is small compared to  $E_\alpha$ , as it always was,  $\sigma$  and  $L$  may be taken as constants over the range of integration and the yield curve looks as shown in Fig. 4B. Over energies from  $E_\alpha$  down to  $E_\alpha - T$ , where  $T$  is the sum of the thicknesses of the target to entrant and emergent ions, the yield curve is approximately,

$$Y(E') = Y_0(E_\alpha - E')/T. \quad (22)$$

One effect of the analyzer energy window will be to round the edges of the distribution as finally observed. If the target thickness is less than the window width, the leading edge of the observed distribution will rise to maximum value in a distance equal to the window width. The point  $E_\alpha$  will correspond to the half-maximum value on the leading edge of the observed distribution in this case. If the target thickness is greater than the window width, the leading edge becomes rounded at the foot and the peak but retains a linear section. The point  $E_\alpha$  will correspond to the extrapolated end point of the linear section of the observed leading edge in this case.

Since the analyzer window energy width is proportional to the energy of the focused ions, the trailing edge of the observed distribution will fall off with the

<sup>20</sup> Neuendorffer, Inglis, and Hanna, Phys. Rev. **82**, 75 (1951).

energy. This effect will be emphasized by the decrease in detector sensitivity with the energy of the focused ions and by the reduced number of charged particles emerging from the target with energies in the lower ranges of the distribution. The predicted form of the curve of counting rate against energy for the alpha-particles from the breakup of Be<sup>8</sup> is shown in Fig. 4C.

The high energy side of the curve in Fig. 4C is not appreciably dependent on the value assumed for the spin of Be<sup>8</sup>. The possible higher values of 2, 4, etc., result in fewer alpha-particles being emitted at right angles to the direction of motion of the Be<sup>8</sup> nucleus but this only affects the alpha-particle spectrum for energies in the middle of the allowed range. The high energy side of the curve in Fig. 4C is not appreciably affected by the width of the ground state of Be<sup>8</sup>, either, since estimates show that the latter is much less than the width of the analyzer energy window.<sup>2,4</sup>

The kevatron ripple does not affect the above analysis since, as an examination of formula (7) shows,

$$dE_{\alpha}/dE_p = \{M_d M_t M_{\alpha} / M_{Be}(M_{Be} + M_d)(M_t + M_p)\} S - M_p M_{\alpha} / (M_p + M_t)^2. \quad (23)$$

With the bombarding energies used in this experiment,  $dE_{\alpha}/dE_p$  is approximately 0.11.

The thickness of a target in the above discussion depends on the relation of the width of the analyzer energy window to the loss of energy of the emergent ions in traversing the beryllium target. The emergent ions in reaction (3) would be Be<sup>8</sup> ions, if their lifetime has the value mentioned in the Introduction, since the beryllium target was no more than 250 angstroms thick and the Be<sup>8</sup> ions should travel about 1000 angstroms before decaying. The emergent ions would be the observed alpha-particles, if the Be<sup>8</sup> lifetime were much shorter than the above value. In either case, the emer-

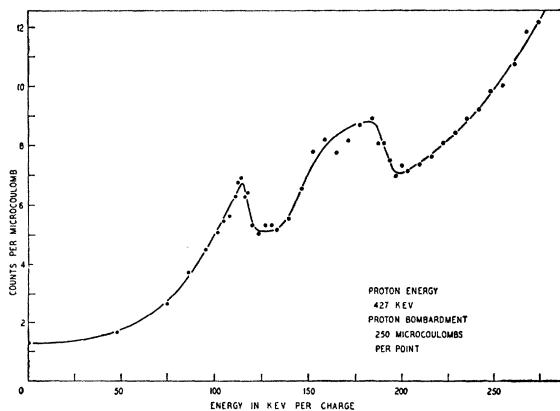


FIG. 5. Observed energy spectrum for 427-keV proton bombardment. The group of particles with an upper energy edge slightly above 200 keV consists of protons from the breakup of stray hydrogen molecular ions striking the target. The doubly-charged alpha-particles from the disintegration of Be<sup>8</sup> have an upper energy edge of 235 keV and appear at an energy-to-charge value of 117 keV per charge.

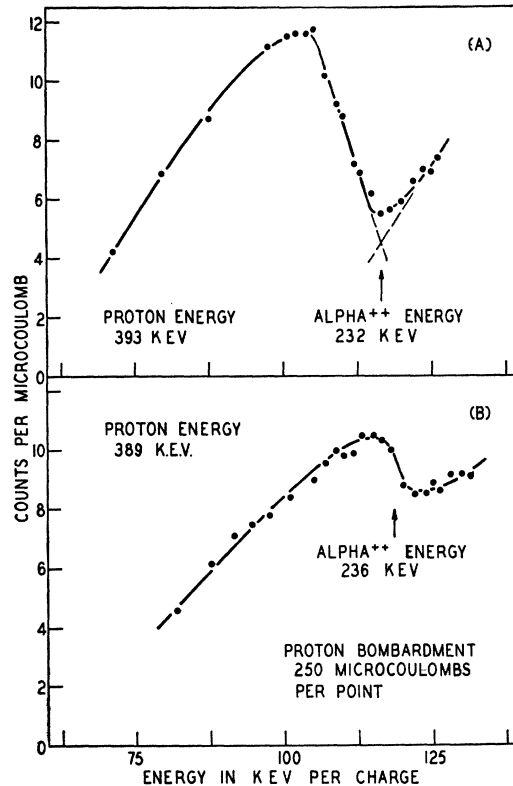


FIG. 6. A. Observed energy spectrum of 393-keV proton bombardment. The doubly-charged alpha-particles from the breakup of Be<sup>8</sup> appear at an energy-to-charge ratio of 116 keV per charge. The target was thick to emergent ions. B. Observed energy spectrum for 389-keV proton bombardment. The double-charged alpha-particles from the breakup of Be<sup>8</sup> appear at an energy-to-charge ratio of 118-keV per charge. The rise occurs in the width of the analyzer energy window. This puts an upper limit on the width of the ground state of Be<sup>8</sup> of 3 keV.

gent ions will lose considerably more energy in any contaminating surface layer on the target than the entrant protons will lose. The latter loss is relatively small and not of great importance since the alpha-particle energy does not depend on the bombarding energy very strongly, as is shown in formula (23). The former loss is of considerable importance, however, since any loss of energy by the emerging ions is directly reflected in the value of the energy release. This is the reason that oil deposition on the target is an important source of error.

## DISCUSSION OF RESULTS

The energy spectrum of the particles obtained by bombarding one of the targets with 427-keV protons is shown in Fig. 5. Only that portion of the spectrum well below the peak due to scattered protons is shown. To understand the difference between this curve and the one in Fig. 4C, one must realize that, while the average thickness of the nickel backing is small enough to confine the elastically scattered protons to a narrow energy band, there is a long tail on the low energy side, probably caused by thick spots on the foil. This tail

TABLE II. Results.

$E_p$ (kev)	$E$ (kev)	$Q_1$ (kev)	Beryllium thickness
$389 \pm 4$	$236 \pm 5$	$80.1 \pm 4$	thin
$393 \pm 4$	$232 \pm 5$	$75.8 \pm 4$	thick
$427 \pm 4$	$235 \pm 5$	$76.5 \pm 4$	thick
Average value = $77.5 \pm 4$			

reaches down to energies of less than 100 kev with a magnitude equal to the counting rate due to the alpha-particles, and can be explained if no more than a few percent of the surface of the backing material is assumed to have thickness two to three times the average thickness. As was mentioned above, this is quite possible considering the method of manufacture.

The peak at the higher energy-to-charge value in Fig. 5 was caused by protons resulting from the breakup of scattered molecular hydrogen ions which managed to get bent into the target chamber. The energy spectrum of the particles from a bare nickel foil, which was bombarded with protons, showed this same peak. Furthermore, the width of the peak, attributed to protons from broken molecular hydrogen ions, is about the same as that of the proton peak shown in Fig. 2 and the position of the former shifts with bombarding energy just as it should if it is due to the presence of molecular hydrogen ions in the beam striking the target. The conclusion is that, in the magnetic analysis of the kevatron beam which was about 60 percent molecular hydrogen ion, the imperfect focusing of the beam and the inhomogeneity of the resolving magnetic field allowed a small amount of molecular ion beam to accompany the proton beam down to the target. From the relative heights of the peaks due to scattered protons and scattered molecules, one can say that about 0.1 percent of the beam striking the target was molecular hydrogen.

The peak at the lower energy-to-charge value in Fig. 5 was attributed to doubly-charged alpha-particles from the breakup of  $\text{Be}^8$ . Figure 6 shows this peak as obtained on two other targets. No peak was obtained, which corresponded to the peak at the lower energy-to-charge value in Figs. 5 and 6, where a bare nickel foil was used as a target with a bombarding energy for protons equal to that used in obtaining the data shown in Fig. 6A.

TABLE III. Energy release in  $\text{Be}^8(\beta, \alpha)\text{Li}^6$  from observed energies of  $\text{Li}^{6++}$  particles.

$E_p$ (kev)	Number of determinations averaged	$E_{\text{Li}}$ (kev)	$Q_1$ (Mev)	Beryllium thickness
$269 \pm 3$	4	$928 \pm 8$	$2.121 \pm 0.020$	thin
$331 \pm 3$	3	$948 \pm 9$	$2.125 \pm 0.023$	thin
$334 \pm 3$	8	$954 \pm 6$	$2.137 \pm 0.014$	thick
Weighted average value = $2.130 \pm 0.010$				

In Figs. 5 and 6A the alpha-particle peak was obtained from thick targets and, in Fig. 6B, it was obtained from a thin target. For a thick target, the proper way to locate the point  $E_\alpha$  is to extrapolate the linear portion of the leading edge of the peak down to a zero counting rate for doubly-charged alpha-particles. The latter is obtained by extrapolation of the falling curve upon which the rise due to doubly-charged alpha-particles is superimposed. These operations have been indicated in Fig. 6. For the data obtained from the thin target, the point  $E_\alpha$  was located by taking it as the position at which half the maximum value of the rise was achieved. The results obtained from the data in Figs. 5 and 6 are listed in Table II. The average of three measurements gives the energy release in the breakup of  $\text{Be}^8$  as 77.5 kev.

The fact that data were obtained from a target which was thin to the emergent ions implies that the width of the ground state of  $\text{Be}^8$  must be less than the width of the analyzer energy window. An upper limit of 3 kev is thereby placed on the width of the ground state of  $\text{Be}^8$ .

The basis of the assignment of the lower peak to alpha-particles from the breakup of  $\text{Be}^8$  was the smallness of the shift in the position of  $E_\alpha$  with the shift in proton bombarding energy. Formula (23) shows this to be a characteristic of the alpha-particles from the breakup. A second reason was the shape of the peak in Fig. 6A. It is quite distinctive and closely approaches the predicted shape for the alpha-particle distribution. Third, there were indications of a peak in the energy spectrum at an energy-to-charge value which was twice that of the lower peak. The singly-charged alpha-particles from the breakup of  $\text{Be}^8$  could have caused these peaks. The number of elastically scattered protons was rising rather sharply at this position and could easily obscure a peak due to the singly-charged alpha-particles. It was for this reason that the peak due to doubly-charged alpha-particles was used to determine the energy release in the breakup of  $\text{Be}^8$ .

Various considerations rule out other assignments for the peak at the lower energy-to-charge value. It cannot be due to singly-charged alpha-particles from the breakup of  $\text{Be}^8$ , since the energy release in the breakup would then be about 6 kev, and the lifetime of  $\text{Be}^8$  would be greater than the age of the earth. Under these circumstances some traces of a stable isotope of beryllium of mass eight ought to have been found. No traces have been found.<sup>3</sup> An assignment of the peak at the lower energy-to-charge value to singly charged alpha-particles also would require the existence of a peak caused by doubly charged alpha-particles at half the energy-to-charge value of the peak observed. No peak was observed at the latter value. The observed peak cannot be the result of a group of particles from either reaction (1), or (2), because the positions in the energy spectrum of the various ions produced are well known and do not fall near the peak in question.<sup>8</sup> Particles

from reaction similar to (1) and (2), in which one of the product ions is left in an excited state, could not cause the peak in question because they would all require larger shifts in the peak position, with changes in the bombarding energy, than the shifts which were observed.

The presence of the elastically scattered protons was a source of trouble in the determination of the point  $E_\alpha$  from the peak due to the doubly-charged alpha-particles since they obscured the high energy side of the peak. The scattering from the molecular ion beam was a similar source of trouble. Targets, which had a relatively large number of thick spots in their backing, would have the peaks due to alpha-particles superposed on a large counting rate due to elastically scattered protons and elastically scattered molecular hydrogen ions. The data were discarded for purposes of determining the point  $E_\alpha$  in these cases. Out of seven targets, on which observations were made, four proved useless for this reason. In the case of those targets which provided useful data, it is felt that the point  $E_\alpha$  was determined with a probable error of 2.0 percent. This estimate of the probable error  $P_\alpha$ , for use in Eq. (14), was obtained by combining the inherent error in the measurement of the energy of a mono-energetic group of particles with the analyzer, the error caused by the finite acceptance angle of the analyzer, and the error caused by the uncertainty in the location of the point  $E_\alpha$ .

In all of the runs to determine the energy release in the Be<sup>8</sup> breakup, there was the danger that carbon would accumulate on the target and slow down the emerging ions. Knowledge of the carbon thickness would be of no help since the energy loss rate and the state of charge of the emergent ions of reaction (3) are not known as functions of the energy. To overcome this difficulty, only fresh targets were used and the position of the peak due to doubly charged Li<sup>6</sup> ions from reaction (1) was determined just before and just after a measurement. In all of the cases reported here, no change of any significance was found. Since Li<sup>6</sup> is a fairly heavy nucleus, it was felt that any carbon accumulation which did not affect it, would not affect the emergent ions of reaction (3).

Considerable data on reaction (1) were compiled in the course of the work. These data are listed in Table III together with estimated errors. The significant points on the peaks caused by Li<sup>6</sup> ions were taken to be the maximum point for the thin targets and the half-maximum point on the leading edge for the thick targets. The classification, as thick or thin, was made on the basis of the Li<sup>6++</sup> peak shape but it always coincided with the classification made on the basis of the shape of the rises caused by the alpha-particles from Be<sup>8</sup>. In observing these lithium peaks, a bombarding energy

TABLE IV. Energy release in Be<sup>8</sup>(p,d)Be<sup>8</sup> from observed deuteron energies.

$E_p$ (kev)	$E_d$ (kev)	$Q_2$ (kev)	Beryllium thickness
202±2	587±6	558±8	thin
202±2	587±6	558±8	thin
202±2	587±6	558±8	thin
202±2	586±6	557±8	thin
Average value = 558±5			

near 331 kev was usually used to take advantage of the resonance in reaction (1) at this energy.<sup>21</sup>

On some of the targets, the peaks in the energy spectrum due to deuterons from reaction (2) were also observed. The deuteron peaks were observed in the same runs that measurements were made to determine the energy release in the breakup. The targets, from which these peaks were obtained, were thick to the emergent ions of reaction (3) and to the Li<sup>6</sup> ions; however, because of their lower energy loss rate, the yield for deuterons was characteristic of a thin target. The results are contained in Table IV. The value of  $Q_2$ , which was used in formula (7), was the average value indicated in the table, 558 kev, with a probable error  $P_2$ , equal to 0.7 percent.

The values of  $Q_1$  and  $Q_2$ , which were mentioned above, agree quite well with the presently accepted values of 2.12 Mev and 560 kev, respectively.<sup>1</sup> Some confidence that serious errors of a systematic nature were not overlooked may be obtained from this agreement. One source of systematic error which such agreement limits is that arising from a deviation of the mean analyzer entrance angle from 90-degrees. From the extent of the agreement between the value of  $Q_1$  obtained here and that presently accepted, it may be seen from formula (8) that the deviation could not be more than 0.016 radian. The correction to  $Q_3$  is less than a kilovolt, therefore, on this account. A kilovolt has been added to the probable error in  $Q_3$ , as calculated from formula (14), to cover this correction. The probable error in  $Q_3$  was calculated with values of 2.0 percent, 0.7 percent, and 1.0 percent for  $P_\alpha$ ,  $P_2$ , and  $P_p$ , respectively. The final estimated probable error in  $Q_3$  is 4 kev, which gives the energy release in the breakup of Be<sup>8</sup> as 77.5±4 kev.

#### ACKNOWLEDGMENTS

The author would like to take this opportunity to thank Professor S. K. Allison for suggesting this problem and for his advice and assistance throughout the course of the work. In addition, he would like to thank the other members of the laboratory, D. Bushnell, H. Casson, H. Kanner, and F. Ribe, for their kind assistance; in particular, he would like to thank H. Kanner for many helpful suggestions.

<sup>21</sup> Thomas, Rubin, Fowler, and Lauritsen, Phys. Rev. **75**, 1612 (1949).

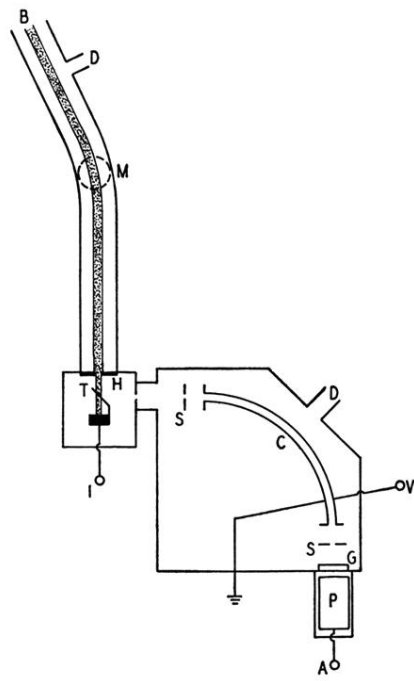


FIG. 1. Schematic diagram of experimental arrangement. A, connection to counting equipment; B, beam from kevatron; C, electrostatic analyzer plates; D, connection to diffusion pump; G, glass disk with zinc sulfide screen; H,  $\frac{1}{8}$ -inch collimating hole; I, connection to beam current integrator; M, magnetic field; P, photomultiplier tube; S, 0.1-cm slit; T, target; V, connection to high voltage.